Acta Biomaterialia 8 (2012) 3261–3269

Contents lists available at SciVerse ScienceDirect

Acta Biomaterialia

journal homepage: www.elsevier.com/locate/actabiomat

Rapidly curable chitosan–PEG hydrogels as tissue adhesives for hemostasis and wound healing

Eugene Lih, Jung Seok Lee, Kyung Min Park, Ki Dong Park *

Department of Molecular Science & Technology, Ajou University, 5 Woncheon, Yeongtong, Suwon 443-749, Republic of Korea

ARTICLE INFO

Article history:
Received 10 January 2012
Received in revised form 23 April 2012
Accepted 1 May 2012
Available online 19 May 2012

Keywords:
Chitosan
Poly(ethylene glycol)
Hydrogel
Tissue adhesive
Hemostasis

ABSTRACT

Chitosan–poly(ethylene glycol)–tyramine (CPT) hydrogels were rapidly formed in situ using horseradish peroxidase and hydrogen peroxide to explore their performance as efficient tissue adhesives. A poly(ethylene glycol) modified with tyramine was grafted onto a chitosan backbone to enhance the solubility of the chitosan and to crosslink into three-dimensional networks. The elastic modulus of the hydrogels could be controlled by changing the crosslinking conditions, and the mechanical strength influenced the tissue adhesiveness of the hydrogels. The hydrogels showed the adhesiveness ranging from 3- to 20-fold that of fibrin glue (Greenplast®). The hemostatic ability of the hydrogels was evaluated on the basis that bleeding from liver defects was significantly arrested by the combined effect of the adhesiveness of the hydrogels and the hemostatic property of the chitosan materials. The enzymatic crosslinking method enabled the water-soluble chitosan to rapidly form hydrogels within 5 s of an incision into the skin of rats. Histological results demonstrated that the CPT hydrogels showed superior healing effects in the skin incision when compared to suture, fibrin glue and cyanoacrylate. By 2 weeks post-implantation, the wound was completely recovered, with a newly formed dermis, due to the presence of the CPT hydrogels in the incision. These results suggest that the in situ curable chitosan hydrogels are very interesting and promising tissue adhesive devices for biomedical applications.

1. Introduction

Tissue adhesives have attracted rapidly growing interest as sealants, hemostatic agents and non-invasive wound-closure devices [1]. The adhesives are required to perform a variety of functions, including sealing leaks, stopping bleeding, binding tissues and preferably facilitating a healing process [2]. Adhesion to biological tissues is a highly challenging task because the adhesive materials should exhibit suitable physical properties (elasticity, tensile and adhesive strength), biocompatibility and biodegradability in contact with physiological fluids. Fibrin glues are widely used as biological tissue adhesives in surgical practices, but sometimes their mechanical property is not sufficient and they are required to be applied on dry substrates [3,4]. Cyanoacrylates are a class of synthetic glues that rapidly solidify upon contact with weak bases (water or blood) and guarantee a high degree of adhesiveness [5]. However, the acrylic derivatives exhibit toxicity, due to aldehydes, which are the degradation products of the glues [6–8]. There have been considerable efforts to develop various synthetic-material-based tissue adhesives (acrylates and poly(ethylene glycol) (PEG) hydrogels), biological adhesives (fibrin glues, polysaccharides and proteins) and hybrid systems [9–13].

One of the prime candidates, chitosan has been used as a wound dressing material due to its superior tissue- or mucoadhesive property, hemostatic activity, low toxicity, relevant biodegradability and anti-infection activity [14–16]. Chitosan is a cationic polysaccharide and its adhesive properties are mainly based on ionic interactions with tissues or mucus layers [17,18]. Low-molecular-weight chitosan is particularly known to facilitate closer interaction with the surface of the epithelial cells [14,19]. Despite the advantages, the rigid crystalline structure of chitosan makes it hard to dissolve in water, and this has partially retarded its potential for such application [20]. Modification of the chitosan with PEG can enhance the water solubility of chitosan and permit the formation of chitosan-based hydrogels by crosslinking of the PEG.

Although in situ forming hydrogels have been suggested as ideal injectable biomaterials, certain properties, like weak mechanical strength, rapid dissolution and cytotoxicity of the hydrogels, need to be considered. Recently, enzyme-mediated in situ crosslinkable hydrogels have received a great deal of attention in tissue engineering because of their tunable mechanical property, rapid gelation time and low toxicity, and the mild crosslinking conditions [21–25]. Park and colleagues reported in situ formation of hydrogels based on tyramine-conjugated Tetronic® or gelatin–PEG via

* Corresponding author. Tel.: +82 31 219 1846; fax: +82 31 219 1592.
E-mail address: kdp@ajou.ac.kr (K.D. Park).

1742-7061/$ - see front matter © 2012 Acta Materialia Inc. Published by Elsevier Ltd. All rights reserved.
http://dx.doi.org/10.1016/j.actbio.2012.05.001

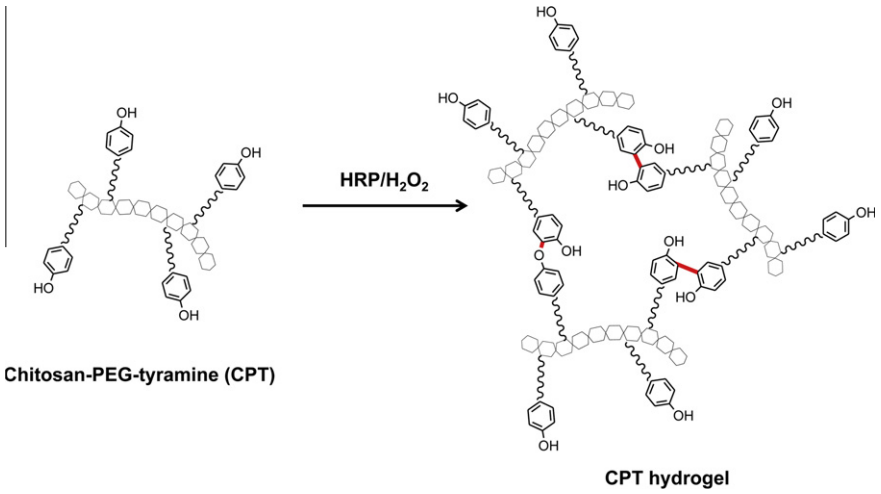

Fig. 1. Schematic representation of in situ gel formation of CPT conjugates using HRP and H_2O_2.

enzymatic oxidative reactions using horseradish peroxidase (HRP) and hydrogen peroxide (H_2O_2) [23–26]. HRP is a hemoprotein that catalyzes the conjugation of phenol and aniline derivatives with decomposed H_2O_2 molecules [27]. The enzymatically crosslinked hydrogels showed excellent bioactivities and tunable physicochemical properties, suggesting that this type of hydrogel has great potential for use as an injectable material for tissue regenerative medicine and various biomedical applications.

In this study, we report on enzyme-triggered in situ formation of hydrogels based on chitosan as a tissue adhesive material for hemostasis and wound healing. For the formation of the hydrogels, chitosan was grafted with tyramine-modified PEGs and the tyramines were crosslinked by HRP and H_2O_2 as shown in Fig. 1. The enzymatic crosslinking enabled the water-soluble chitosan to rapidly form hydrogels, which stably adhered to the wound site for a desired period of time. The hydrogels were characterized in terms of their physicomechanical properties, such as gelation time, elastic moduli and adhesive strengths, under various conditions. The hemostatic and adhesive properties of the hydrogels as well as the wound healing capability were also evaluated in vivo.

2. Materials and methods

2.1. Materials

Chitosan (low molecular weight, 75–85% deacetylated), poly(ethylene glycol) (4000 g mol^{-1}), HRP (units per mg solid (using pyrogallol)), hydrogen peroxide, 4-dimethylamino pyridine (DMAP) and p-nitrophenylchloroformate (PNC) were purchased from Sigma–Aldrich (St. Louis, MO). Tyramine (TA) was purchased from Acros Organics. Triethylamine (TEA) and aluminum oxide were obtained from Kanto Chemical Co. and Strem Chemicals, respectively. Fibrin glue kit (Greenplast®) was purchased from Green Cross Co. and *n*-butyl-2-cyanoacrylate adhesive (Histoacryl®) was obtained from Tissueseal, LLC (Ann Arbor, MI, USA). For cell culture, Dulbecco's modified Eagle's medium (high glucose), fetal bovine serum, trypsin/ethylenediaminetetraacetic acid, penicillin–streptomycin and phosphate-buffered saline (PBS, pH 7.4) were obtained from Gibco BRL (Carlsbad, CA). Fluorescein diacetate and ethidium bromide were purchased from Sigma–aldrich. A Cell Counting Kit-8 was purchased from Dojindo (Kumamoto, Japan). All other chemicals and solvents were used such without further purification.

2.2. Synthesis of chitosan–poly(ethylene glycol)–tyramine (CPT) conjugates

The CPT conjugates were synthesized according to the previously reported method [23]. Amine-reactive PEG (PNC–PEG–PNC) was prepared by activating the hydroxyl groups of PEG with excess of PNC. The activated PEG was reacted with TA and subsequently with chitosan, to form the CPT conjugates (Fig. 2). Briefly, PEG (10 g, 5 mmol of hydroxyl groups) was dissolved in methylene chloride (MC, 100 ml) at room temperature under a nitrogen atmosphere.

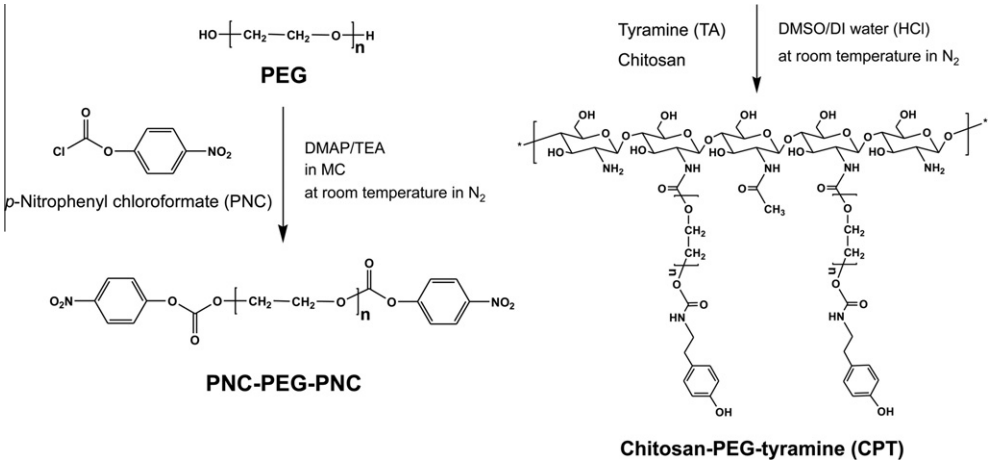

Fig. 2. Synthetic route of the CPT conjugates. Preparation of (a) PNC–PEG–PNC and (b) the conjugation of the PNC–PEG–TA with chitosan.

A solution of DMAP (0.916 g, 7.5 mmol) and TEA (0.759 g, 7.5 mmol) dissolved in MC (20 ml) was added to the PEG solution. The mixed solution was stirred at room temperature for 15 min for the activation of the terminal hydroxyl groups. The mixture was then slowly added to a solution of MC (50 ml) containing PNC (1.511 g, 7.5 mmol) in a dropwise manner. The reaction was carried out for 24 h at room temperature under N_2. The resulting solution was evaporated and precipitated in cold diethyl ether. The precipitate was filtered and dried under vacuum to obtain the PNC–PEG–PNC conjugates.

The CPT conjugates were prepared by coupling a chemically modified PEG to a chitosan backbone. PNC–PEG–PNC (4 g, 2 mmol of PNC groups) was dissolved in dimethyl sulfoxide (DMSO, 50 ml) at room temperature under a nitrogen atmosphere. A solution of TA (0.137 g, 1 mmol) dissolved in DMSO (25 ml) was added dropwise to the PNC–PEG–PNC solution, and reacted for 6 h under a nitrogen atmosphere to prepare mono-TA-conjugated PEG (PNC–PEG–TA). Chitosan (0.2 g) was dissolved in a co-solvent of dilute hydrochloric acid solution (3 ml, pH 5) and DMSO (300 ml), and the PNC–PEG–TA solution was added to the chitosan solution. The mixture was stirred at room temperature under a nitrogen atmosphere for 24 h. After completion of the reaction, the solution was subjected to filtration using an aluminum oxide pad to remove PNC salt, followed by dialysis (with a molecular weight cut-off of 12–14 kDa, SpectraPor®) against 0.01 M PBS solution (pH 7.4) for 3 days and then in distilled water for 2 days. The dialyzed solution was lyophilized to obtain the CPT conjugates in the form of a white powder.

The chemical structures of PNC–PEG–PNC and CPT were characterized by ^{1}H nuclear magnetic resonance (NMR) spectroscopy (Varian, 400 MHz spectrometer). The degree of substitution of the TA groups was measured at a wavelength of 275 nm with an ultraviolet (UV)–visible spectrometer (V-750 UV/VIS/NIR, Jasco, Japan). The concentration of conjugated TA groups in the CPT conjugates was calculated from the standard curve obtained by monitoring the absorbance of a known concentration of TA in deionized water. The chitosan and PEG compositions in the CPT conjugates were evaluated by thermogravimetric analysis (TGA), using a TGA Q50 analyzer (TA Instrument, USA). The experiment was carried out under a nitrogen atmosphere with a heating rate of 10 °C min^{-1} in the temperature range from 30 to 800 °C.

2.3. Gelation time measurements and rheological analysis

CPT hydrogels at a polymer concentration of 10 wt.% were dissolved in HRP solution (0.002–0.063 mg ml^{-1} of stock solution) and H_2O_2 solution (0.06 wt.% of stock solution) in 0.01 M PBS (pH 7.4), and mixed under mild stirring. The gelation times of the hydrogels were determined using the vial-tilting method [22]. The gel state was regarded as the condition when no flow was observed within a minute after inversion of the vial. The experiments were performed in triplicate.

Rheological experiments (elastic modulus, G′) were carried out with an Advanced Rheometer GEM-150–050 (Bohlin Instruments, USA) using the parallel plates (20 mm diameter) configuration at 37 °C in oscillatory mode. The CPT polymers were dissolved both in HRP solution (0.06 mg ml^{-1} of stock solution) and in solutions containing different concentrations of H_2O_2 (0.015–0.06 wt.% of stock solution). The polymer solutions containing HRP and H_2O_2 were rapidly mixed on the bottom plate of the rheometer and the upper plate was immediately lowered down to a measuring gap size of 1 mm. A frequency of 0.1 Hz (single frequency) and a strain of 0.1% (strain control) were applied for the analysis to maintain the linear viscoelastic response.

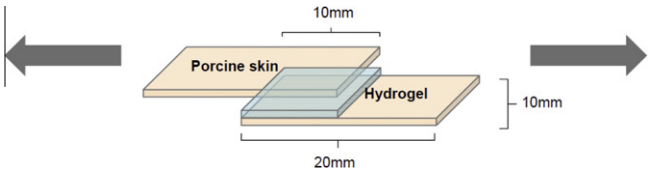

Fig. 3. Schematic illustration of the measurement of tissue adhesive strength.

2.4. Tissue adhesive strength

The adhesive properties were assessed by the following procedures, and are shown in Fig. 3. According to the method modified from ASTM F2255–05 [28,29], the tissue adhesive strength of the CPT hydrogels was measured using a universal testing machine (Instron Model 3343, Norwood, MA, USA) at different H_2O_2 concentrations. Sections of porcine skin, used as substrates for the experiment, were cut and cleaned to remove any excess fat. The CPT solutions (10 wt.%) were dissolved in an HRP solution (0.06 mg ml^{-1} of stock solution) and H_2O_2 solutions (0.015–0.06 wt.% of stock solution). The HRP solution was applied on one surface of the porcine skin (bonding area: 10×10 mm^2) and the specimen was immediately covered with another tissue specimen treated with the H_2O_2 solutions. During the test, the overlapped skins were kept at room temperature for 30 min in a humid environment. The bonded skins were loaded until complete separation was achieved at a crosshead speed of 10 mm min^{-1} with a 100 N load cell. Measurements were performed on 20 samples of CPT hydrogels in order to reduce the experimental error rate. Fibrin glue was also measured under the same conditions as a control adhesive ($n = 5$).

2.5. In vivo hemostatic ability test

To evaluate the hemostatic potential of the CPT hydrogels, a hemorrhaging liver mouse model was employed (C57BL/6 mouse, 22–25 g, 5 weeks, male) [30–32]. All animal studies were performed in compliance with guidelines set by national regulations and were approved by the local animal experiments ethical committee. Briefly, a mouse was anesthetized using zoletil and fixed on a surgical corkboard. The liver of the mouse was exposed by abdominal incision, and serous fluid around the liver was carefully removed to prevent inaccuracies in the estimation of the blood weight obtained by the filter paper. A pre-weighted filter paper on a paraffin film was placed beneath the liver. Bleeding from the liver was induced using a 20 G needle with the corkboard tilted at about 30° and 50 μl of hydrogel was immediately applied to the bleeding site using the dual syringe kit filled with the CPT solutions (“A” solution: 5 wt.% of CPT in an HRP solution (0.06 mg ml^{-1}); “B” solution: 5 wt.% of CPT in a H_2O_2 solution (0.06 wt.%)). After 3 min, the weight of the filter paper with absorbed blood was measured and compared with a control group (no treatment after pricking the liver).

2.6. Animal experiment for wound closure

All animal studies were performed in compliance with guidelines set by national regulations and were approved by the local animal experiments ethical committee. To evaluate the bioadhesive property and the biocompatibility of the CPT hydrogels, rats (normal SD rat, 100–150 g, 4 weeks, male) were anesthetized using zoletil and their backs were shaved. Skin incisions 1.5 cm long and skin thickness deep were made on both sides of the rat’s back [33]. The skin incisions were quickly closed by suture, fibrin glue, cyanoacrylate and CPT hydrogels. For this study, the CPT hydrogels were

prepared similarly to the hemostatic experiments. The hydrogels were sterilized by filtration using 200 nm syringe filters and prepared with the dual syringe kit. A 50 μl aliquot of hydrogels was applied to the wound area. At 7 and 14 days post-implantation, the closure skin was harvested and fixed in *p*-formaldehyde solution (3.7 wt.%) for histological analysis by hematoxylin and eosin (H&E) stain.

3. Results and discussion

3.1. Synthesis of CPT conjugates

The CPT conjugates were prepared by grafting PNC–PEG–TA onto chitosan backbones. PNC–PEG–PNC was synthesized and coupled with TA prior to the grafting. The PNC conjugation ratio in the PEG chains was approximately 98% (molar ratio of PEG and PNC ~1:2), as previously reported [23]. The degree of TA conjugation with the PEG was calculated by ^{1}H NMR spectroscopy, and it was found that 97% of PEG in the CPT conjugates was functionalized with TA. The TA content in the CPT conjugates was also determined by UV measurements (275 nm) and the TA content was calculated to be ~180 μmol g^{-1} of CPT (data not shown). The weight ratio of chitosan and PEG in the CPT conjugates was determined by TGA (Fig. 4b). It was confirmed that the chitosan to PEG ratio was 3:7 (w/w). The conjugate gave the following ^{1}H NMR peaks in D_2O: δ 1.86 (COCH3, chitosan), δ 3.5–3.8 (ethylene groups of PEG) and δ 6.68 and 7.00 (aromatic protons of TA).

3.2. Rapid gelation time of CPT hydrogels

The CPT hydrogels were prepared by the simple blending of prefabricated polymer and enzyme solutions. In general, the in situ preparation of the hydrogels takes about 5 s at an HRP concentration of 0.063 mg ml^{-1}. A fast in situ gelation is essential in order to quickly cover the defect surface and subsequently crosslink into the hydrogels, which can adhere tightly to the bleeding surface (typical gelation time of fibrin glues: 5 s). In contrast, very rapid gelation can also result in the formation of non-homogeneous hydrogels, which will result in insufficient mechanical properties and adhesiveness. Notably, homogeneous and transparent CPT hydrogels were formed under mild conditions, and no phase separation was observed. The gelation time of the CPT hydrogels could be adjusted by changing the amount of the enzymes and the polymer concentration used for the preparation. Fig. 5 shows the gelation time of the CPT hydrogels with increasing concentrations of CPT as a function of the amount of HRP. The HRP solutions containing CPT copolymer (10 wt.%) were mixed with H_2O_2 solution (0.03 wt.%). The final concentrations of HRP were from 0.002 to 0.063 mg ml^{-1}. A faster gelation time was obtained when more HRP was involved in the crosslinking reactions, as the rate of the

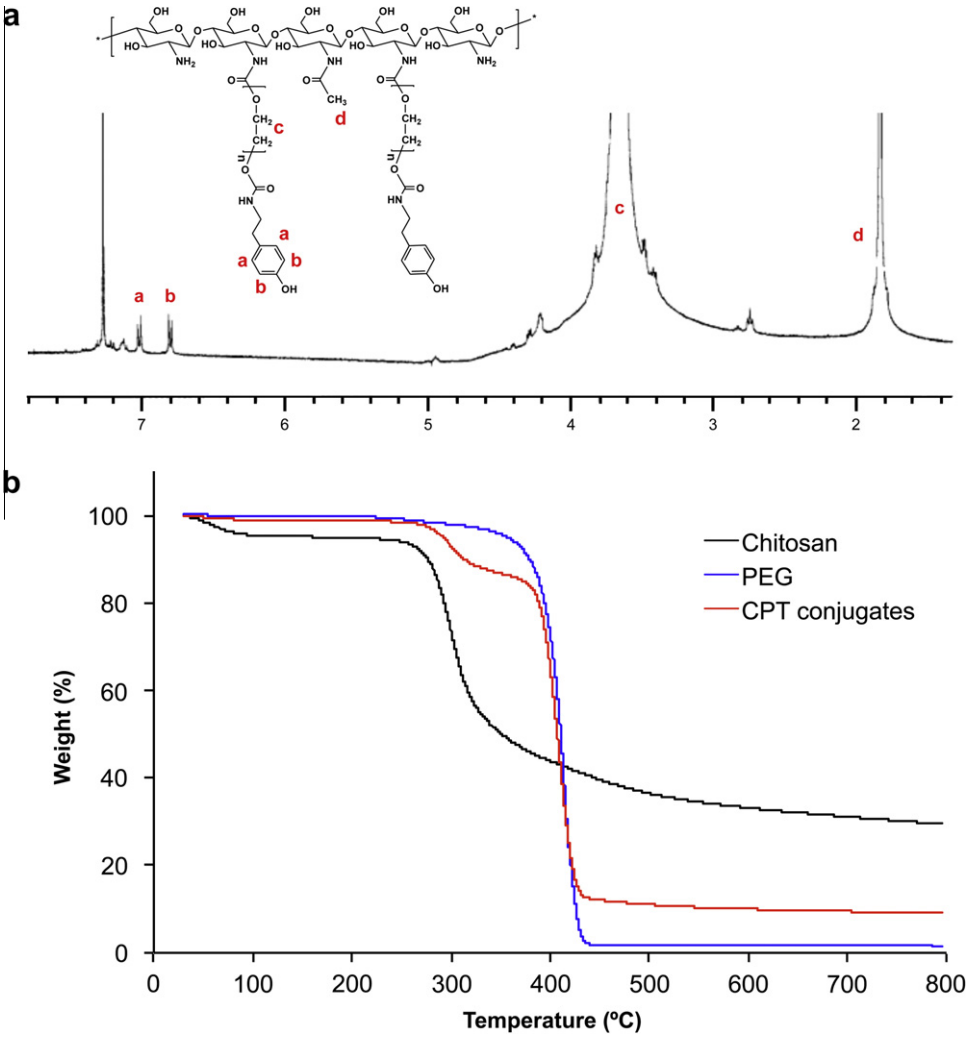

Fig. 4. Characterizations of CPT conjugates: (a) ^{1}H NMR spectrum and (b) TGA curves.

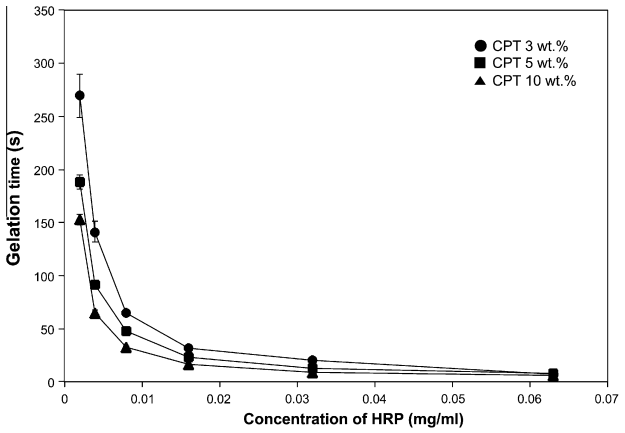

Fig. 5. Gelation time of CPT hydrogels with respect to different CPT concentrations, depending on the amount of HRP used for the reactions (0.002–0.063 mg ml^{-1}) (n = 5, mean ± SD).

formation of phenoxy radical was accelerated due to the high concentration of HRP. The radicals reacted with hydroxyl groups or *ortho*-carbons of phenol groups in the CPT. The effect of CPT concentration on gelation time was significant at the lowest HRP concentration, but became negligible at higher concentrations.

3.3. Tunable mechanical property

The elastic moduli of the chitosan-based hydrogels were studied by oscillatory rheology experiments of polymer solutions containing HRP and H_2O_2 in PBS at 37 °C. The concentrations of the CPT conjugates, H_2O_2, and HRP used in the formation of the CPT hydrogels are listed in Table 1, and the change in the elastic modulus value of the CPT hydrogels is presented in Fig. 6. After mixing the reactant solutions, there was a quick increase in the elastic modulus in time due to the rapid enzymatic crosslinking reactions. The plateau value reached was the G' value, indicating the end of the crosslinking process. The elastic modulus of the CPT hydrogels could be controlled by changing the crosslinking conditions, e.g. the concentration of H_2O_2. At an HRP concentration of 0.06 mg ml^{-1}, the elastic modulus was about 8 kPa when 0.06 wt.% of H_2O_2 was used, and this value decreased with decreasing H_2O_2 concentration. This is because HRP catalyzes the conjugation of phenol groups with decomposed H_2O_2 molecules, and it is assumed that H_2O_2 at less than 0.06 wt.% is not enough to fully crosslink the hydrogels.

3.4. High tissue adhesive strength

The adhesive strength of the CPT hydrogels was assessed at different H_2O_2 concentrations using the modified ASTM F2255–05 method, which is a standard test method for evaluating he strength properties of tissue adhesives in lap-shear by tension loading [28,29]. The CPT hydrogels were prepared using the same conditions as used for the rheological studies (Table 1). Porcine skins were used as the substrate materials (bonding area: 10×10 mm^2) and fibrin glue was used as the control bioadhesive. None of the skin portions became unattached before the end of the tests. When the tissue skins were sliding in different directions, separation of two skins occurred due to the cohesion failure of the hydrogels. This phenomenon could explain the relationship between the adhesive strength and the elastic modulus of the CPT hydrogels. The hydrogels with an elastic modulus of 8 kPa showed an adhesive strength of 97 kPa, whereas 17 kPa of adhesiveness was obtained for the CPT hydrogels with an elastic modulus of 0.5 kPa. A higher mechanical strength led to a higher adhesive strength. It is conceivable that the bulk property of the CPT hydrogels is correlated to the cohesive strength required to sustain a given amount of strain. In this case, the bonding between tissue and adhesives could be relatively stable but the sample could be prone to cohesive failure. This explanation is consistent with the previous observations that fibrin sealants with a high elastic modulus failed through an adhesive mode, while the fibrins with low stiffness primarily failed through a cohesive mode [34].

Interestingly, the CPT hydrogels exhibited adhesiveness ranging from 3- to 20-fold that for the fibrin glue used in the study (Greenplast®). The adhesive strength of the fibrin glue was about 5 kPa, whereas it was 17–97 kPa for the CPT hydrogels (Fig. 7). The adhesive properties of chitosan have been attributed mainly to the interaction between its positively charged amino groups with negatively charged sialic acid groups present on the mucus membrane [35]. It has also been reported that chitosan interacts with the phospholipids of cell membranes mainly through electrostatic interactions, including hydrogen bonding and hydrophobic forces, depending on the phospholipid packing density [36]. These factors appear to affect the extent of the response to chitosan, including the degree of acetylation and the molecular weight of chitosan, which could facilitate closer interaction of chitosan with the surface of epithelial cells [14]. Several reports have also shown that chitosan and other cationic polymers are able to interact with tight junctions in different epithelial cells, yielding a reversible opening and reorientation of the tight junction without any permanent cell damage [14,19]. The general consensus regarding this variable appears to be that a degree of deacetylation of more than 80% has the greatest effect on cells [19]. However, it is still not

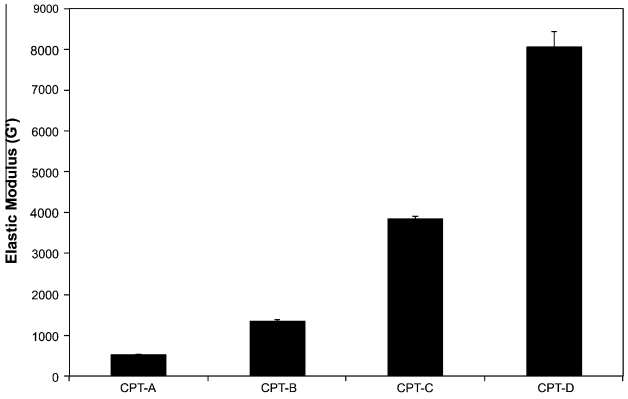

Fig. 6. Elastic moduli (G') of CPT hydrogels (10 wt.%) depending on the different concentrations of H_2O_2.

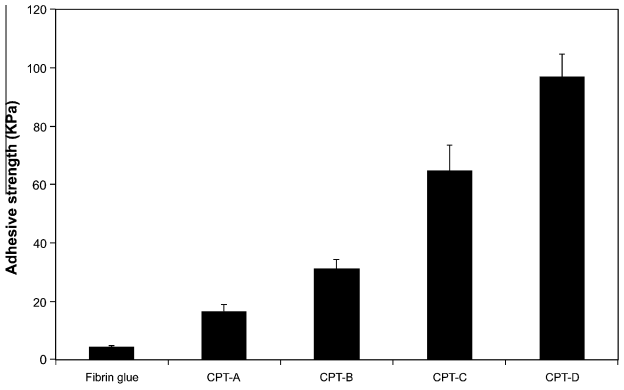

Fig. 7. Adhesive strength of CPT hydrogels on porcine tissues (n = 20, mean ± SD). The adhesiveness of fibrin glue was compared with that of the hydrogels.

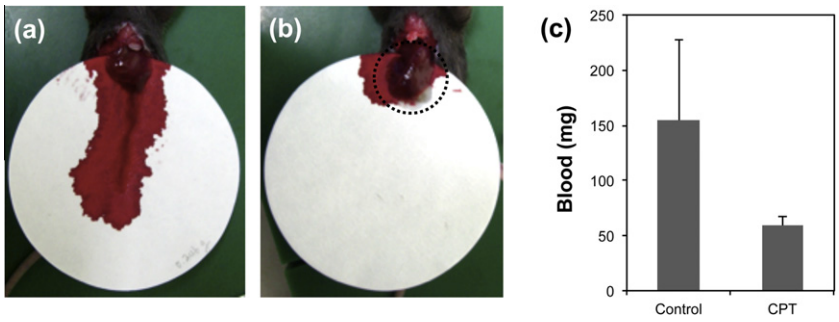

Fig. 8. The evaluation of hemostatic ability of the hydrogel: (a) control and (b) CPT-D hydrogels. (c) Total blood loss from the damaged livers after 3 min. The black circle denotes the CPT hydrogels sealing the liver (n = 3, mean ± SD).

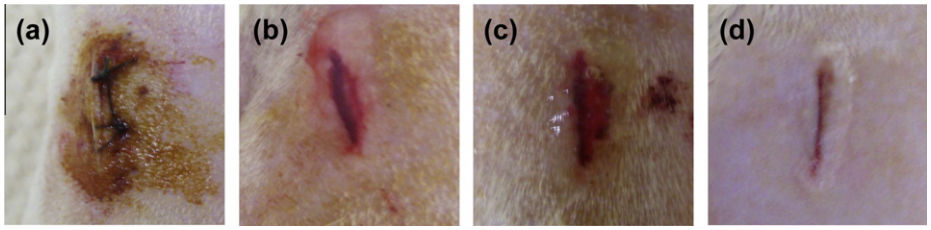

Fig. 9. Photographs of wound closures. Skin incisions on back of the rats were treated by (a) suture, (b) fibrin glue, (c) CPT-D hydrogels and (d) cyanoacrylate.

clear how the intrinsic nature of chitosan imparts strong adhesive properties at the molecular level.

3.5. Excellent hemostatic property of CPT hydrogels

Hemostatic agents are widely applied on hemorrhaging sites of tissues or organs during intra-abdominal surgery [2,30,31]. Many materials have been studied for their ability to arrest bleeding, but they are not always effective in hemostasis; for example, the agent should be in the liquid form before application and must rapidly solidify in the presence of body fluid with similar pliability as of the damaged organs or tissues. In this study, CPT hydrogels were explored as hemostatic tissue adhesives based on their previously reported excellent adhesive properties [37]. Fig. 8a and b show photographs of untreated bleeding liver and the extent of bleeding after the application of hydrogels onto the liver, respectively. The total blood loss from the control liver was about 154 mg for 3 min after the liver was pricked with a needle. In contrast, the bleeding was significantly arrested by the dressing of hydrogels, the loss of blood being reduced to 59 mg through the combined effect of the adhesiveness of the hydrogels and the hemostatic property of chitosan (Fig. 8c). This result demonstrates that the CPT hydrogels exhibit both elastic and adhesive properties when crosslinked in situ, thus serving as an effective anti-hemorrhaging agent.

3.6. CPT hydrogels as wound closure materials

Recently, there has been an increase in the use of non-invasive wound closure devices to avoid the pain of suturing and to lessen the inconvenience caused to the patient [12,13]. Attractive alternatives to sutures and staples are required to rapidly adhere to the skin close to the wound edges and to keep the wound closed for a sufficient time, preferably with biodegradability, tissue regenerative property and minimal toxicity. To explore the use of CPT-D hydrogels as wound closure devices, skin incisions on the backs of rats were treated with CPT hydrogels and compared with suture-, fibrin glue- and cyanoacrylate-treated models, as well as normal skins. Fig. 9 presents photographs of the skin incisions just after these treatments. Complete closure of the skin defect was observed for the suture and cyanoacrylate models. The CPT hydrogels showed a small gap between the two edges of tissue, though the size of the gap was less than in the case of the fibrin glue.

Table 1
Concentrations of CPT conjugates, H_2O_2, and HRP used in the enzymatic crosslinking reactions for the formation of CPT hydrogels.

	CPT (wt.%)	H_2O_2 (wt.%)	HRP (mg ml^{-1})
CPT-A	10	0.015	0.06
CPT-B	10	0.030	0.06
CPT-C	10	0.045	0.06
CPT-D	10	0.060	0.06

At 7 and 14 days after implantation, the skin samples were harvested and observed by H&E staining. Fig. 10 shows the H&E-stained histology of cross-sections of normal skin and skin defects sealed by suture, fibrin glue, cyanoacrylate and CPT-D hydrogel at 7 and 14 days post-wounding. In Fig. 10b, a large gap is apparent at the incision site in the suture model and blood clots can be seen at the point of application of the suture thread. After 14 days, the epidermal layer has penetrated into the sutured incision and the large gap still remains, together with a suture hole (Fig. 10g). Cyanoacrylate performed much better with respect to wound closure than suturing, although the gap was still present where the cyanoacrylate was applied (Fig. 10d). Fig. 10i reveals that the incision had still not been completely crossed by newly formed collagen after 14 days, and the healing process was incomplete, demonstrating fibrosis around the incision.

The fibrin glue-covered incision exhibited enhanced wound healing when compared to the sutured and cyanoacrylate-covered incisions at 14 days post-wounding. However, fibrosis was still observed, with incomplete dermis recovery. Compared with the other three kinds of adhesive glue, CPT-D hydrogels showed superior

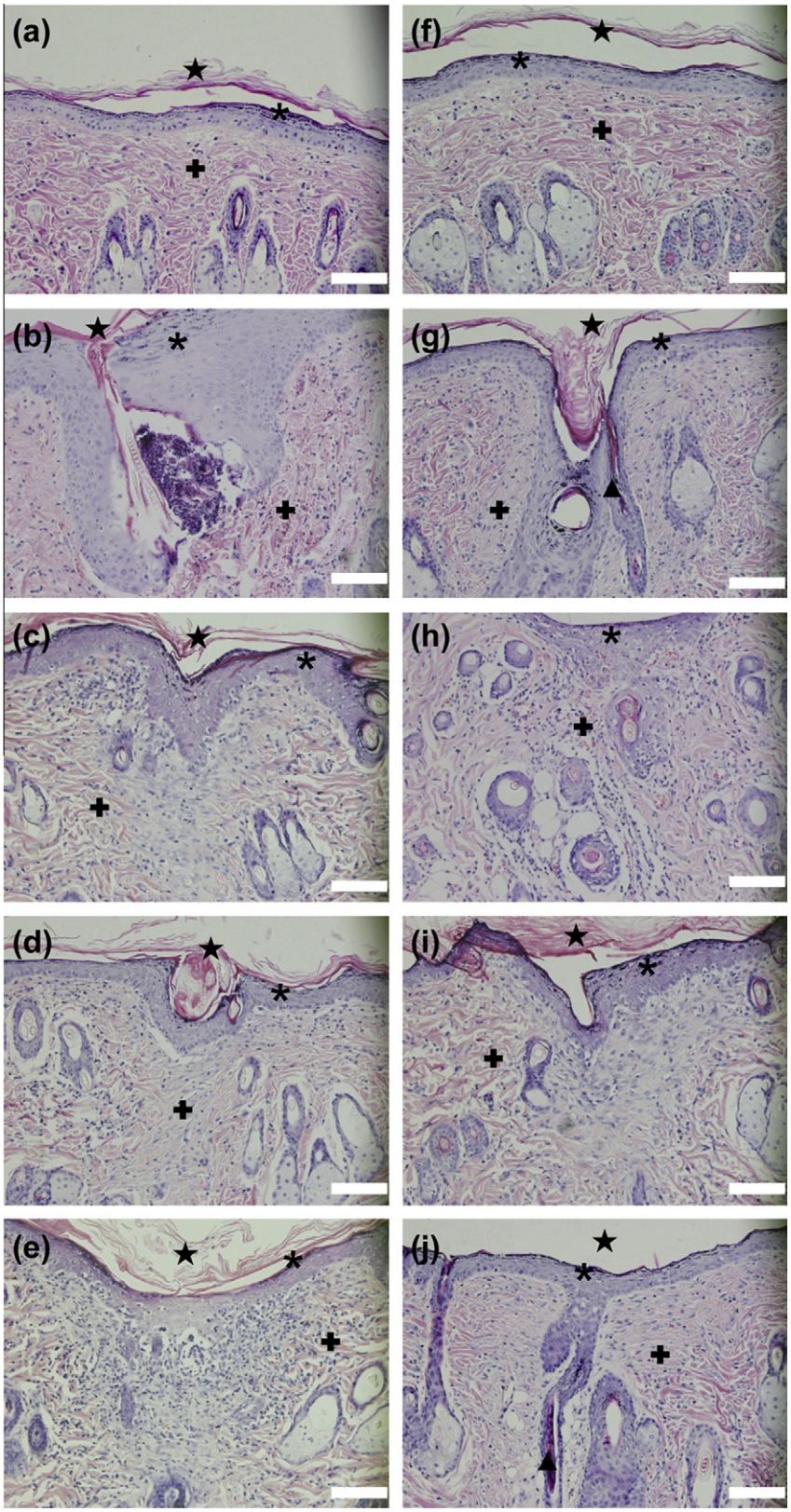

Fig. 10. H&E histological examination of CPT-D hydrogel (a–e) 7 and (f–j) 14 days after implantation, respectively; (a, f) normal tissue, (b, g) suture, (c, h) fibrin glue, (d, i) cyanoacylate and (e, j) CPT-D hydrogel. Stratum corneum (★), epidermis (*), dermis (×), and hair follicle (▲) are presented. Size bars are 100 μm.

healing effects on the incision (Fig. 10e and j). The incision was completely recovered, with a newly formed dermis and no visible fibrosis, after 2 weeks. This observation can be explained by the fact that chitosan improves the healing of the wound [14–16]. It is known that chitosan evokes a minimal foreign body reaction, with little or no fibrous encapsulation, acceleration of normal

granulation tissue formation, angiogenesis or rapid dermal regeneration [17,18]. Kim et al. reported that chitosan influenced all stages of wound repair in experimental animal models [17].

Normally, chitosan-based hydrogels slowly degrade after several months in vitro [38]. However, the rate of the degradation in wound fluid would be much faster due to the secretion of overexpressed and up-regulated lysozymes from the wound site. It has been reported that the concentration of lysozyme in the wound fluid is more than 0.5 mg ml^{-1} and the activity is 376 ± 240 U ml^{-1}, while it is even higher in the infected wound (4830 ± 1848 U ml^{-1}) [39–41]. For all materials, no sign of inflammation or infection in the incisions was observed in this study.

4. Conclusions

Bioadhesive hydrogels based on chitosan were fabricated for use as potential tissue adhesive materials. Enzyme-mediated in situ crosslinking of hydrogels was performed using chitosan grafted with PEG via HRP/H_2O_2. The mechanical strength as well as the adhesiveness of the hydrogels was adjustable by using different concentrations of H_2O_2. This tunable adhesiveness makes the hydrogels suitable as efficient bioadhesives in various medical applications, which require a different range of adhesive strengths. When applied to a rat liver defect or a rat skin incision model, hydrogels cured by the enzymatic crosslinking method showed excellent hemostatic properties and wound healing effects within 5 s. We propose that in situ curable chitosan hydrogels are useful as bioadhesives for numerous medical applications. In a future investigation, mechanistic studies on the strong tissue adhesiveness of the chitosan hydrogels will be performed in the molecular level. Moreover, the in vivo degradation of hydrogels in various tissue defects will also be evaluated.

Acknowledgements

This work was supported by the National Research Foundation of Korea (NRF) Grant funded by the Korea government (MEST) (2010-0027776), Nano-Biotechnology Project (Regenomics), Ministry of Science & Technology (2011-0007746 (B020214)), and the Korea Science and Engineering Foundation, Ministry of Education, Science and Technology (2011-0001805).

Appendix A. Figures with essential colour discrimination

Certain figures in this article, particularly Figs. 1, 3, 4, 8, 9 and 10, are difficult to interpret in black and white. The full colour images can be found in the on-line version, at http://dx.doi.org/10.1016/j.actbio.2012.05.001.

Appendix B. Supplementary data

Supplementary data associated with this article can be found, in the online version, at http://dx.doi.org/10.1016/j.actbio.2012.05.001.

References

[1] Reece TB, Maxey TS, Kron IL. A prospectus on tissue adhesives. Am J Surg 2001;182:S40–4.
[2] Spotnitz WD, Burks S. Hemostats, sealants, and adhesives: components of the surgical toolbox. Transfusion 2008;48:1502–16.
[3] MacGillivray TE. Fibrin sealants and glues. J Card Surg 2003;18:480–5.
[4] Sierra DH. Fibrin sealant adhesive systems: a review of their chemistry, material properties and clinical applications. J Biomater Appl 1993;7:309–52.
[5] Mobley SR, Hilinski J, Toriumi DM. Surgical tissue adhesives. Facial Plast Surg Clin North Am 2002;10:147–54.
[6] Leggat PA, Smith DR, Kedjarune U. Surgical applications of cyanoacrylate adhesives: a review of toxicity. ANZ J Surg 2007;77:209–13.
[7] Singer AJ, Quinn JV, Hollander JE. The cyanoacrylate topical skin adhesives. Am J Emerg Med 2008;26:490–6.
[8] Eaglstein WH, Sullivan T. Cyanoacrylates for skin closure. Dermatol Clin 2005;23:193–8.
[9] Chen Q, Liang S, Thouas GA. Synthesis and characterisation of poly(glycerol sebacate)-co-lactic acid as surgical sealants. Soft Matter 2011;7:6484–92.
[10] Chen T, Janjua R, McDermott MK, Bernstein SL, Steidl SM, Payne GF. Gelatin-based biomimetic tissue adhesive. Potential for retinal reattachment. J Biomed Mater Res Part B: Appl Biomater 2006;77B:416–22.
[11] Lee Y, Chung HJ, Yeo S, Ahn C-H, Lee H, Messersmith PB, et al. Thermo-sensitive, injectable, and tissue adhesive sol–gel transition hyaluronic acid/pluronic composite hydrogels prepared from bio-inspired catechol–thiol reaction. Soft Matter 2010;6:977–83.
[12] Oelker AM, Grinstaff MW. Ophthalmic adhesives: a materials chemistry perspective. J Mater Chem 2008;18:2521–36.
[13] Ryou M, Thompson CC. Tissue adhesives: a review. Tech Gastrointest Endosc 2006;8:33–7.
[14] Ibrahim AA. Chitosan topical gel formulation in the management of burn wounds. Int J Biol Macromol 2009;45:16–21.
[15] Jayakumar R, Prabaharan M, Sudheesh Kumar PT, Nair SV, Tamura H. Biomaterials based on chitin and chitosan in wound dressing applications. Biotechnol Adv 2011;29:322–37.
[16] Ueno H, Mori T, Fujinaga T. Topical formulations and wound healing applications of chitosan. Adv Drug Deliv Rev 2001;52:105–15.
[17] Kim I-Y, Seo S-J, Moon H-S, Yoo M-K, Park I-Y, Kim B-C, et al. Chitosan and its derivatives for tissue engineering applications. Biotechnol Adv 2008;26:1–21.
[18] Sezer A, Hatipoglu F, Cevher E, Oğurtan Z, Bas A, Akbuğa J. Chitosan film containing fucoidan as a wound dressing for dermal burn healing: preparation and in vitro/in vivo evaluation. AAPS Pharm Sci Tech 2007;8:E94–E101.
[19] Smith J, Wood E, Dornish M. Effect of chitosan on epithelial cell tight junctions. Pharm Res 2004;21:43–9.
[20] Park JH, Cho YW, Chung H, Kwon IC, Jeong SY. Synthesis and characterization of sugar-bearing chitosan derivatives: aqueous solubility and biodegradability. Biomacromolecules 2003;4:1087–91.
[21] Jin R, Hiemstra C, Zhong Z, Feijen J. Enzyme-mediated fast in situ formation of hydrogels from dextran–tyramine conjugates. Biomaterials 2007;28:2791–800.
[22] Kurisawa M, Chung JE, Yang YY, Gao SJ, Uyama H. Injectable biodegradable hydrogels composed of hyaluronic acid-yramine conjugates for drug delivery and tissue engineering. Chem Commun 2005;43:12–4.
[23] Park KM, Ko KS, Joung YK, Shin H, Park KD. In situ cross-linkable gelatin–poly(ethylene glycol)–tyramine hydrogel via enzyme-mediated reaction for tissue regenerative medicine. J Mater Chem 2011;21:13180–7.
[24] Park KM, Shin YM, Joung YK, Shin H, Park KD. In situ forming hydrogels based on tyramine conjugated 4-arm-PPO–PEO via enzymatic oxidative reaction. Biomacromolecules 2010;11:706–12.
[25] Tran NQ, Joung YK, Lih E, Park KD. In situ forming and rutin-releasing chitosan hydrogels as injectable dressings for dermal wound healing. Biomacromolecules 2011;12:2872–80.
[26] Park KM, Jun I, Joung YK, Shin H, Park KD. In situ hydrogelation and RGD conjugation of tyramine-conjugated 4-arm PPO–PEO block copolymer for injectable bio-mimetic scaffolds. Soft Matter 2011;7:986–92.
[27] Lee F, Chung JE, Kurisawa M. An injectable hyaluronic acid–tyramine hydrogel system for protein delivery. J Control Release 2009;134:186–93.
[28] Kull S, Martinelli I, Briganti E, Losi P, Spiller D, Tonlorenzi S, et al. Glubran2 surgical glue: in vitro evaluation of adhesive and mechanical properties. J Surg Res 2009;157:e15–21.
[29] Ninan L, Monahan J, Stroshine RL, Wilker JJ, Shi R. Adhesive strength of marine mussel extracts on porcine skin. Biomaterials 2003;24:4091–9.
[30] Liu Y, Kopelman D, Wu L-Q, Hijji K, Attar I, Preiss-Bloom O, et al. Biomimetic sealant based on gelatin and microbial transglutaminase: an initial in vivo investigation. J Biomed Mater Res Part B: Appl Biomater 2009;91B:5–16.
[31] Murakami Y, Yokoyama M, Nishida H, Tomizawa Y, Kurosawa H. In vivo and in vitro evaluation of gelation and hemostatic properties of a novel tissue-adhesive hydrogel containing a cross-linkable polymeric micelle. J Biomed Mater Res Part B: Appl Biomater 2009;91B:102–8.
[32] Ryu JH, Lee Y, Kong WH, Kim TG, Park TG, Lee H. Catechol-functionalized chitosan/pluronic hydrogels for tissue adhesives and hemostatic materials. Biomacromolecules 2011;12:2653–9.
[33] Mo X, Iwata H, Ikada Y. A tissue adhesives evaluated in vitro and in vivo analysis. J Biomed Mater Res Part A 2010;94A:326–32.
[34] Serrero Al, Trombotto Sp, Bayon Y, Gravagna P, Montanari S, David L. Polysaccharide-based adhesive for biomedical applications: correlation between rheological behavior and adhesion. Biomacromolecules 2011;12:1556–66.
[35] Fiebrig I, Harding S, Davis S. Sedimentation analysis of potential interactions between mucins and a putative bioadhesive polymer ultracentrifugation. Prog Colloid Polym Sci 1994;94:66–73.
[36] Pavinatto FJ, Pavinatto A, Caseli L, dos Santos DS, Nobre TM, Zaniquelli MED, et al. Interaction of chitosan with cell membrane models at the air–water interface. Biomacromolecules 2007;8:1633–40.
[37] Samyn P, Ruhe Jr, Biesalski M. Polymerizable biomimetic vesicles with controlled local presentation of adhesive functional DOPA groups. Langmuir 2010;26:8573–81.
[38] Shi C, Zhu Y, Ran X, Wang M, Su Y, Cheng T. Therapeutic potential of chitosan and its derivatives in regenerative medicine. J Surg Res 2006;133:185–92.

[39] Choi JS, Yoo HS. Pluronic/chitosan hydrogels containing epidermal growth factor with wound-adhesive and photo-crosslinkable properties. J Biomed Mater Res Part A 2010;95A:564–73.
[40] Frohm M, Gunne H, Bergman A-C, Agerberth B, Bergman T, Boman A, et al. Biochemical and antibacterial analysis of human wound and blister fluid. Eur J Biochem 1996;237:86–92.
[41] Hasmann A, Wehrschuetz-Sigl E, Kanzler G, Gewessler U, Hulla E, Schneider KP, et al. Novel peptidoglycan-based diagnostic devices for detection of wound infection. Diagn Microbiol Infect Dis 2011;71:12–23.